HHS Public Access

Author manuscript

Bioconjug Chem. Author manuscript; available in PMC 2019 April 18.

Published in final edited form as:

Bioconjug Chem. 2018 April 18; 29(4): 878–884. doi:10.1021/acs.bioconjchem.7b00757.

Combination of heparin binding peptide and heparin cell surface coatings for mesenchymal stem cell spheroid assembly

Jennifer Lei[†,¥], **William L. Murphy**[‡,#], and **Johnna S. Temenoff**[§,¥,*]

[†]The George W. Woodruff School of Mechanical Engineering, Georgia Tech, Georgia 30332, United States

[‡]Department of Biomedical Engineering, University of Wisconsin-Madison, Wisconsin 53706, United States

[#]Department of Orthopedics and Rehabilitation, University of Wisconsin-Madison, Wisconsin 53705, United States

[§]Coulter Department of Biomedical Engineering, Georgia Tech/Emory University, Georgia 30332, United States

[¥]Parker H. Petit Institute for Bioengineering and Bioscience, Georgia Tech, Georgia 30332, United States

Abstract

Microtissues containing multiple cell types have been used in both *in vitro* models and *in vivo* tissue repair applications. However, to improve through-put, there is a need to develop a platform that supports self-assembly of a large number of 3D microtissues containing multiple cell types in a dynamic suspension system. Thus, the objective of this study was to exploit the binding interaction between the negatively charged glycosaminoglycan, heparin, and a known heparin binding peptide to establish a method that promotes assembly of mesenchymal stem cell (MSC) spheroids into larger aggregates. We characterized heparin binding peptide (HEPpep) and heparin coatings on cell surfaces and determined the specificity of these coatings in promoting assembly of MSC spheroids in dynamic culture. Overall, combining spheroids with both coatings promoted up to 70±11% of spheroids to assemble in to multi-aggregate structures, as compared to only 10±4% assembly when cells having the heparin coating were cultured with cells coated with a scrambled peptide. These results suggest that this self-assembly method represents an exciting approach that may be applicable for a wide range of applications in which cell aggregation is desired.

Table of Contents Figure

[*] *to whom correspondence should be addressed:* johnna.temenoff@bme.gatech.edu.

Associated Content

Supporting Information

Additional detailed materials and methods. Supplemental figures showing control populations and confocal imaging.

The authors declare no competing financial interest.

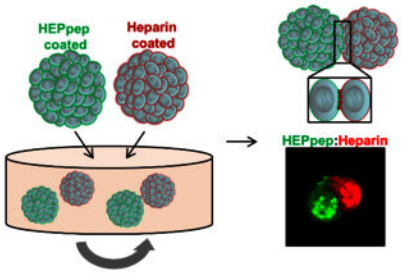

Introduction

Microtissues formed from smaller tissue constructs or cells have been used in both *in vitro* models and *in vivo* tissue repair applications.[1,2] Microtissue models can recapitulate tumor or tissue microenvironments for drug screening and have been typically executed in cellular arrays or microfluidic devices that provide a means to culture cells in either two-dimensions or three-dimensions (3D).[2–5] For tissue repair purposes, assembled 3D microtissues aim to recapitulate multiple aspects of complex physiological microenvironments for efficient integration, both functionally and morphologically, with the defect tissue.[6–8]

To create microtissues with multiple cell types, current methods include encapsulation in hydrogels, scaffold-free technologies, and microfluidic devices. Hydrogel encapsulation has been used to control organization of cell populations by encapsulating different cell types into separate sections or seeding all cell types in a mixed population in one single hydrogel.[9–11] Scaffold-free technologies utilize centrifugation or gravity to force cells into an aggregate form. In this approach, multiple cell types are typically mixed together and cultured together in one aggregate.[12,13] Lastly, microfluidic systems have been used to form high throughput arrays of small microtissues. Spatial organization of different cell types is typically achieved by introducing different cell types into the small specialized devices sequentially to allow for each cell type to interact and bind with each other.[14–17]

While these methods have all shown have the ability to produce multicellular microtissues, there are disadvantages to each of these approaches. In encapsulation and scaffold-free technologies, formation is typically performed at a single microtissue scale, in which one hydrogel or one aggregate is produced at a time.[11,18] While microfluidic devices have the ability to produce multiple microtissues simultaneously,[2,3,15] the number formed is limited by the number of devices that need to be used. Another shortcoming is that formation of microtissues with multiple cell types requiring physical placement of different populations adjacent to each other often require external biomaterials, such as hydrogels or microparticles, or specialized devices, such as microfluidic devices, to support assembly.[10,19] Finally, previous methods have typically developed microtissues under static conditions, as opposed to dynamic culture, that can provide mixing and diffusion of nutrients and oxygen to promote higher viability of the cells within the microtissue construct.[8]

Given the limitations of current microtissue assembly technologies, the long-term goal of this work is to develop a platform that supports simultaneous self-assembly of a large number of 3D microtissues containing multiple cell types in a dynamic suspension system. As a step toward this goal, MSC spheroids were chosen as the model cell type in these studies because these cells have been extensively used in numerous microtissue applications, including cartilage, hepatic, vascularized tissues and bone marrow niches.[8,20–23] To achieve self-assembly, we utilized a cell coating that has been previously developed in our laboratory that uses layer-by-layer technology using biotin, and avidin to graft a biotinylated glycosaminoglycan (GAG), heparin, onto cell surfaces prior to formation of small spheroids.[24] Heparin (Hep) is a negatively charged naturally derived polysaccharide that is known to interact with growth factors such as fibroblast growth factor-2 (FGF-2).[25,26] Specific heparin binding sites have been identified on FGF-2, and one of these sequences has been synthesized into a short sequence known as a heparin binding peptide (HEPpep). This peptide has been previously used as part of a self-assembled monolayer that is able to specifically sequester heparin from culture media.[27,28]

Thus, the objective of this study was to investigate the use of HEPpep and heparin coatings on assembly of small aggregates of MSCs (MSC spheroids) into larger microtissues in a dynamic 3D culture system (see Figure 1). We examined the utility of these coatings in promoting assembly of MSC spheroids in dynamic, rotary culture and determined the relative specificity of this interaction by comparing cellular assembly between HEPpep/heparin coatings vs. assembly with the use of either a scrambled peptide coating (Scramble) or a desulfated heparin coating (Hep-). In particular, it was hypothesized that the interaction between HEPpep and heparin would result in greater cellular assembly compared to interactions involving the scrambled peptide (same overall net charge and amino acid composition, but different sequence) [27], or the desulfated heparin coating (less overall negative charge [29].

Results and Discussion

In preliminary studies, confocal imaging (Figure 2) revealed that, by using a layer-by-layer coating procedure (see schematic in Figure 1), biotinylated HEPpep peptide and biotinylated natively sulfated heparin (Hep) were grafted on cell surfaces and did not disturb spheroid formation. Biotinylated fully desulfated heparin (Hep-) can also be grafted onto cell surfaces of spheroids and has been visualized for up to 14 days.[30]

At day 1 and day 3 after coating, both fluorescently tagged HEPpep and Hep were visualized in red on cell surfaces throughout the entire spheroid (Figure 2A-B, D-E). Additionally, LIVE/DEAD staining revealed that after 3 days, coated cells in spheroids remained viable (Figure 2C-F). While other systems have grafted the HEPpep sequence to 2D surfaces,[27] this is the first reported example of grafting this peptide sequence onto cell surfaces

For the cellular aggregation studies, assembly of spheroids with a HEPpep coating can occur in two forms: culture in environments containing soluble GAGs or culture with Hep coated spheroids (see Figure 1). To quantify the specificity of the HEPpep coating and its effects on

spheroid assembly, coated spheroids were cultured in media containing soluble GAG and the diameter of all spheroids in each population was measured. After 24 hours, none of the control populations (noncoated cultured in the presence of soluble GAG and coated spheroids cultured by themselves) exhibit spheroid assembly and the average diameter of each population was not significantly different from each other (Figure S1). Measurements from these control populations were used to establish a cut-off diameter that were utilized in the analysis of spheroid assembly (see Methods section and Figure S1),

In further studies examining the effects of soluble GAGs in the media, it was observed that only HEPpep coated spheroids formed larger constructs when cultured in media containing soluble Hep or Hep- (Figure 3; 34±6% for Hep or 37±5% for Hep- of the entire population had diameters larger than the cutoff size). In contrast, percentage of population with spheroids larger than the cutoff size was not significantly different than the control population when HEPpep coated spheroids were cultured in basal (no GAG) media (6±5%) or when Scrambled-coated spheroids were cultured under any conditions (13±7% in Hep, 10±2% in Hep-, and 8±6% in basal) (Figure 3C-F, Table 1).

Because HEPpep presents a sequence specific for heparin binding, we believe that soluble Hep can act as a crosslinker to bring together these HEPpep coated spheroids while in rotary culture. This specific interaction has been observed previous reports that have shown that HEPpep grafted to a 2D surface is able to sequester heparin from culture supplements.[27] Contrary to our hypothesis, the similar results observed with Hep- in the media indicates that Hep- may retain a similar enough 3D structure to interact with HEPpep to form larger assembled spheroids. While 3D conformation is likely affected through sulfate group removal, exactly how that affects the GAG sequence recognition by HEPpep remains unclear.[31] However, the general concept of specific interaction between HEPpep and heparin derivatives is supported by data using the scrambled peptide that has the same level of positive charge as the HEPpep sequence but does not express a specific heparin binding site, which did not promote assembly.

In subsequent experiments, the assembly of spheroid populations with different coatings was also observed to be specific to HEPpep–Hep interactions. In these studies, the peptide-coated cells were tagged with CellTracker Orange (Molecular Probes) so assembly could be tracked (Figure 4). When HEPpep coated spheroids were cultured with Hep coated spheroids, the percentage of aggregates with diameters above the cutoff size was 70±11%, which was significantly greater than the percentage calculated in control populations containing noncoated spheroids or coated spheroids cultured without binding partners. Interestingly, when the ratio of HEPpep coated spheroids to Hep coated spheroids in culture was varied, at the ratio of 10:1, no assembly of spheroids was observed over 24 hours. This may indicate a ratio (10-fold excess of one of the spheroid types) at which no assembly of different spheroid populations will occur due to a lack of sufficient partner molecules for binding (Figure S2).

Additionally, 27±4% of the spheroids had larger diameters when HEPpep coated spheroids were cultured with Hep- coated spheroids, which was also significantly higher compared to the control groups. However, percentages of larger aggregates when HEPpep and Hep-

coated groups were cultured together were significantly less than when HEPpep and Hep groups were co-cultured (Table 2). This, combined with the data from Figure 3, indicates that, while there is some interaction between the HEPpep and Hep- coatings, it likely does not have the same affinity as the interaction between HEPpep and Hep coatings. This is in accordance with previous findings that that specific GAG sulfation locations (N- and 2-O) are required for FGF-2 binding and activation.[30,32] Therefore, it would be expected that interaction with HEPpep, which is derived from a heparin binding site of FGF-2, would be reduced upon heparin desulfation.

Examining other combinations, only 12±5% of the spheroids was greater than cutoff size when HEPpep coated spheroids were cultured with noncoated spheroids (Table 2). When Scrambled coated spheroids were cultured with the Hep coated, Hep- coated or noncoated spheroids, 10±4%, 9±6%, and 6±2% of each population, respectively, had diameters above the cutoff size, all of which were not significantly different when compared to the control populations containing noncoated spheroids and coated spheroids cultured by themselves (Figure 4C-F, Table 2), further indicating that it is the interaction between the GAG and HEPpep coatings that drives multi-spheroid aggregate formation in this system.

To date, this is the first reported study of microtissue assembly from smaller MSC building blocks in a dynamic system of culture. However, we have identified certain limitations in this system that will need to be further addressed in future work. While only one cell type was used in this study, we have previously shown the ability to assemble coated spheroids using different cell types,[24,33,34] facilitating future development of multicellular microtissues that can be cultured for tissue model or repair applications. Additionally, in these studies, we demonstrated that while assembly can occur between HEPpep and Hep coated spheroids at efficiencies of up to 70%, further control over the relative cellular composition of aggregates formed may be necessary. Specifically, further examination of this system is required to determine the effect of altering the ratio of cells of each population, the size of the spheroid to be assembled, and rotation speed during dynamic culture, on the cellular composition of the aggregates formed. This system also does not address cellular rearrangement that may occur after aggregation, which may eventually result in mixing of the cells within the larger assembly.[18,35] Finally, long-term function of the assembled organoids, including cellular differentiation, should be assessed.

Conclusions

We have shown in these studies that, by exploiting the ability of heparin to bind to particular peptide sequences, microtissues can be built by smaller building block aggregates in suspension, and that this interaction is specific, with the combination of fully sulfated heparin and HEPpep coatings resulting in the greatest aggregation. The dynamic nature of the culture system in which assembly occurs represents a technology that is amenable to large scale up bioprocesses, an aspect that has not been previously addressed in microtissue research. Thus, this self-assembly method represents an exciting technology that may be amenable to a wide range of applications in which cell aggregation is desired, from in *in vitro* tissue modeling to *in vivo* tissue repair applications.

Materials and Methods

MSC expansion

MSCs derived from human bone marrow aspirates were obtained from the Texas A&M Health Sciences Center and cultured using established protocols.[24,30] For details, see supplemental information.

Materials synthesis

Desulfation of heparin was performed via acidic methanol treatment for 6 days, as previously published,[29] and conjugated with biotin as per.[30] Biotinylated HEPpep (Biotin-NH_2-$(CH_2)_4$-GKRTGQYKLG-NH_2) and biotinylated Scramble peptide (Biotin-NH_2-$(CH_2)_4$-GTYRKKGLQG-NH_2) were both purchased from Aapptec, Louisville, KY. Alexa-Fluor 633 conjugation to HEPpep and heparin was performed by EDC coupling in 0.1 M sodium bicarbonate buffer containing 10 mg/mL HEPpep or heparin, 10mM AlexaFluor® −633-hydrazide (Invitrogen), 20 μM EDC.[30] See supplementary information for more details on materials synthesis.

MSC coating and spheroid formation

HEPpep and heparin coating and spheroid formation was performed as previously published, [24,30] (see supplementary information for details). Assembly of coated spheroids were performed either by incubating coated spheroids in media containing soluble GAG or by incubating GAG-coated and peptide-coated spheroids together (see supplemental information for details). For all experiments, spheroids were cultured for 24 hours on rotary at 65rpm, after which, samples were collected, fixed with 10% neutral buffered formalin and imaged under phase microscopy (Inverted Nikon TE 200 microscope). For cell viability studies, at days 1 and 3 after coating, spheroids were collected, washed in PBS and stained with LIVE/DEAD staining solution (calcein AM at 1 μM and ethidium homodimer-1 at 1 μM, Invitrogen) and imaged under confocal microscopy at excitation wavelength 494 nm and emission wavelength of 517 nm.

Statistical analysis

To determine % spheroids assembled, the diameters that were determined at the upper 5% of the population for all control groups were averaged and set as the cutoff size. For experimental groups, the cutoff size was applied to each population and the percentage of measured diameters above that size was reported. The sub-population of diameters for each group that was larger than the cutoff size was statically compared using a one-way analysis of variance with Tukey's post hoc multiple comparisons test ($p<0.05$) in Minitab (v.15.1).

To compare the percentages, the resampling method of bootstrapping was used to produce variance for each population.[36,37] Bootstrap resampling was performed in MATLAB and 900 diameters were chosen at random from the original population to create a new set of measurements. This was performed three times to create triplicates for each experimental group. Percentage of diameters above the cutoff size from each resampled population was then determined. Average percentages for each experimental group was calculated and

statistically compared using a one-way analysis of variance with Tukey's post hoc multiple comparisons test ($p<0.05$) to determine statistical difference between groups in Minitab.

Supplementary Material

Refer to Web version on PubMed Central for supplementary material.

Acknowledgements

The authors would like to acknowledge Dr. Tobias Miller and Dr. Yifeng Peng for assistance with heparin material synthesis. The human MSCs employed in these studies were provided by the Texas A&M Health Science Center College of Medicine Institute for Regenerative Medicine at Scott & White through a grant from NCRR of the NIH, Grant #P40RR017447. This work was supported by an NSF DMR (1207045) grant awarded to JST, and grants from the National Institutes of Health (R01HL093282) and Environmental Protection Agency (835737) to WLM.

References

1. Kelm JM and Fussenegger M (2010) Scaffold-free cell delivery for use in regenerative medicine. Advanced drug delivery reviews. 62, 753–64.20153387
2. Kim JY , Fluri DA , Marchan R , Boonen K , Mohanty S , Singh P , Hammad S , Landuyt B , Hengstler JG , Kelm JM , et al. (2015) 3d spherical microtissues and microfluidic technology for multi-tissue experiments and analysis. Journal of biotechnology. 205, 24–35.25592049
3. van Midwoud PM , Verpoorte E and Groothuis GM (2011) Microfluidic devices for in vitro studies on liver drug metabolism and toxicity. Integrative biology : quantitative biosciences from nano to macro. 3, 509–21.21331391
4. Toh YC , Lim TC , Tai D , Xiao G , van Noort D and Yu H (2009) A microfluidic 3d hepatocyte chip for drug toxicity testing. Lab on a chip. 9, 2026–35.19568671
5. Yoon No D , Lee K-H , Lee J and Lee S-H (2015) 3d liver models on a microplatform: Well-defined culture, engineering of liver tissue and liver-on-a-chip. Lab on a chip. 15, 3822–3837.26279012
6. Fennema E , Rivron N , Rouwkema J , van Blitterswijk C and de Boer J (2013) Spheroid culture as a tool for creating 3d complex tissues. Trends in biotechnology. 31, 108–15.23336996
7. Kelm JM and Fussenegger M (2004) Microscale tissue engineering using gravity-enforced cell assembly. Trends in biotechnology. 22, 195–202.15038925
8. Lin RZ and Chang HY (2008) Recent advances in three-dimensional multicellular spheroid culture for biomedical research. Biotechnology journal. 3, 1172–84.18566957
9. Hammoudi TM , Rivet CA , Kemp ML , Lu H and Temenoff JS (2012) Three-dimensional in vitro tri-culture platform to investigate effects of crosstalk between mesenchymal stem cells, osteoblasts, and adipocytes. Tissue engineering. Part A. 18, 1686–97.22472084
10. Rinker TE , Hammoudi TM , Kemp ML , Lu H and Temenoff JS (2014) Interactions between mesenchymal stem cells, adipocytes, and osteoblasts in a 3d tri-culture model of hyperglycemic conditions in the bone marrow microenvironment. Integrative biology : quantitative biosciences from nano to macro. 6, 324–37.24463781
11. Maia FR , Fonseca KB , Rodrigues G , Granja PL and Barrias CC (2014) Matrix-driven formation of mesenchymal stem cell-extracellular matrix microtissues on soft alginate hydrogels. Acta biomaterialia. 10, 3197–208.24607421
12. Bhatia SN , Balis UJ , Yarmush ML and Toner M (1998) Probing heterotypic cell interactions: Hepatocyte function in microfabricated co-cultures. Journal of Biomaterials Science, Polymer Edition. 9, 1137–1160.9860177
13. Bhatia SN , Yarmush ML and Toner M (1997) Controlling cell interactions by micropatterning in co-cultures: Hepatocytes and 3t3 fibroblast. Journal of Biomedical Materials Researh. 34, 187–199.
14. Beachley VZ , Wolf MT , Sadtler K , Manda SS , Jacobs H , Blatchley MR , Bader JS , Pandey A , Pardoll D and Elisseeff JH (2015) Tissue matrix arrays for high-throughput screening and systems analysis of cell function. Nature methods. 12, 1197–1204.26480475

15. Gallego-Perez D , Higuita-Castro N , Sharma S , Reen RK , Palmer AF , Gooch KJ , Lee LJ , Lannutti JJ and Hansford DJ (2010) High throughput assembly of spatially controlled 3d cell clusters on a micro/nanoplatform. Lab on a chip. 10, 775–82.20221567

16. Otsuka H (2010) Nanofabrication of nonfouling surfaces for micropatterning of cell and microtissue. Molecules. 15, 5525–46.20714311

17. Legant WR , Pathak A , Yang MT , Deshpande VS , McMeeking RM and Chen CS (2009) Microfabricated tissue gauges to measure and manipulate forces from 3d microtissues. Proceedings of the National Academy of Sciences of the United States of America. 106, 10097–102.19541627

18. Napolitano A , Dean D , Man A , Youssef J , Ho D , Rago A , Lech M and Morgan J (2007) Scaffold-free three-dimensional cell culture utilizing micromolded nonadhesive hydrogels. BioTechniques. 43, 494–500.18019341

19. Bratt-Leal AM , Kepple KL , Carpenedo RL , Cooke MT and McDevitt TC (2011) Magnetic manipulation and spatial patterning of multi-cellular stem cell aggregates. Integrative biology : quantitative biosciences from nano to macro. 3, 1224–32.22076329

20. Kelm JM , Breitbach M , Fischer G , Odermatt B , Agarkova I , Fleischmann BK and Hoerstrup SP (2012) 3d microtissue formation of undifferentiated bone marrow mesenchymal stem cells leads to elevated apoptosis. Tissue engineering. Part A. 18, 692–702.21988679

21. Kelm JM , Djonov V , Ittner L , Fluri DA , Born W , Hoerstrup SP and Fussenegger M (2006) Design of custom-shaped vascularized tissues using microtissue spheroids as minimal building units. Tissue Engineering. 12, 2151–2160.16968156

22. Futrega K , Palmer JS , Kinney M , Lott WB , Ungrin MD , Zandstra PW and Doran MR (2015) The microwell-mesh: A novel device and protocol for the high throughput manufacturing of cartilage microtissues. Biomaterials. 62, 1–12.26010218

23. Zhao F (2013) Manipulation mesenchymal stem cells for vascular tissue engineering. JSM Biotechnology and Biomedical Engineering. 1, 1012–1015.

24. Lei J , McLane LT , Curtis JE and Temenoff JS (2014) Characterization of a multilayer heparin coating for biomolecule presentation to human mesenchymal stem cell spheroids. Biomaterials science. 2, 666–673.25126416

25. Baird A , Schubert D , Ling N and Guillemin R (1988) Receptor- and heparin-binding domains of basic fibroblast growth factor. PNAS 85, 2324–2328.2832850

26. Bellosta P , Iwahori A , Plotnikov AN , Eliseenkova AV , Basilico C and Mohammadi M (2001) Identification of receptor and heparin binding sites in fibroblast growth factor 4 by structure-based mutagenesis. Molecular and Cellular Biology. 21, 5946–5957.11486033

27. Hudalla GA , Koepsel JT and Murphy WL (2011) Surfaces that sequester serum-borne heparin amplify growth factor activity. Advanced materials. 23, 5415–8.22028244

28. Koepsel JT and Murphy WL (2012) Patterned self-assembled monolayers: Efficient, chemically defined tools for cell biology. Chembiochem : a European journal of chemical biology. 13, 1717–24.22807236

29. Seto SP , Miller T and Temenoff JS (2015) Effect of selective heparin desulfation on preservation of bone morphogenetic protein-2 bioactivity after thermal stress. Bioconjugate chemistry. 26, 286–93.25621929

30. Lei J , Trevino E and Temenoff J (2016) Cell number and chondrogenesis in human mesenchymal stem cell aggregates is affected by the sulfation level of heparin used as a cell coating. Journal of biomedical materials research. Part A. 104, 1817–29.26990913

31. Ashikari-Hada S , Habuchi H , Kariya Y , Itoh N , Reddi AH and Kimata K (2004) Characterization of growth factor-binding structures in heparin/heparan sulfate using an octasaccharide library. The Journal of Biological Chemistry. 279, 12346–12354.14707131

32. Lundin L , Larsson H , Kreuger J , Kanda S , Lindahl U , Salmivirta M and Claesson-Welsh L (2002) Selectively desulfated heparin inhibits fibroblast growth factor-induced mitogenicity and angiogenesis. Journal of Biological Chemistry. 275, 24653–24660.

33. Cabric S , Sanchez J , Johansson U , Larsson R , Nilsson B , Korsgren O and Magnusson PU (2010) Anchoring of vascular endothelial growth factor to surface-immobilized heparin on

pancreatic islets: Implications for stimulating islet angiogenesis. Tissue Engineering: Part A. 16, 961–970.20021270

34. Wilson JT , Haller CA , Qu Z , Cui W , Urlam MK and Chaikof EL (2010) Biomolecular surface engineering of pancreatic islets with thrombomodulin. Acta biomaterialia. 6, 1895–903.20102751
35. Napolitano AP , Chai P , Dean DM and Morgan JR (2007) Dynamics of the self-assembly of complex cellular aggregates on micromolded nonadhesive hydrogels. Tissue Eng. 13, 2087–94.17518713
36. Anselme K and Bigerelle M (2006) Modelling approach in cell/material interaction studies. Biomaterials. 27, 1187–1199.16257051
37. Bigerelle M and Anselme K (2005) Bootstrap analysis of the relation between initial adhesive events and long-term cellular functions of human osteoblasts cultured on biocompatible metallic substrates. Acta biomaterialia. 1, 499–510.16701830

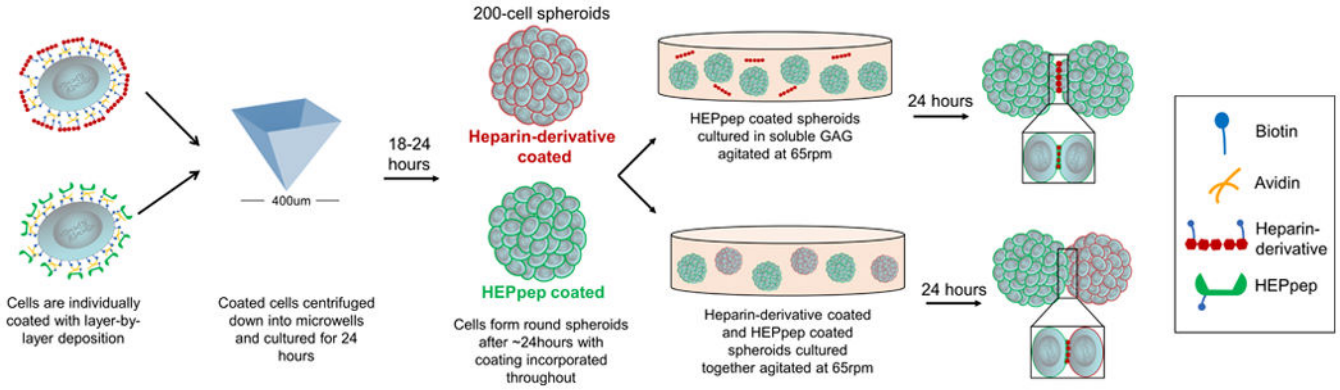

Figure 1.
Schematic of layer-by-layer coating procedure, spheroid formation, and spheroid assembly.

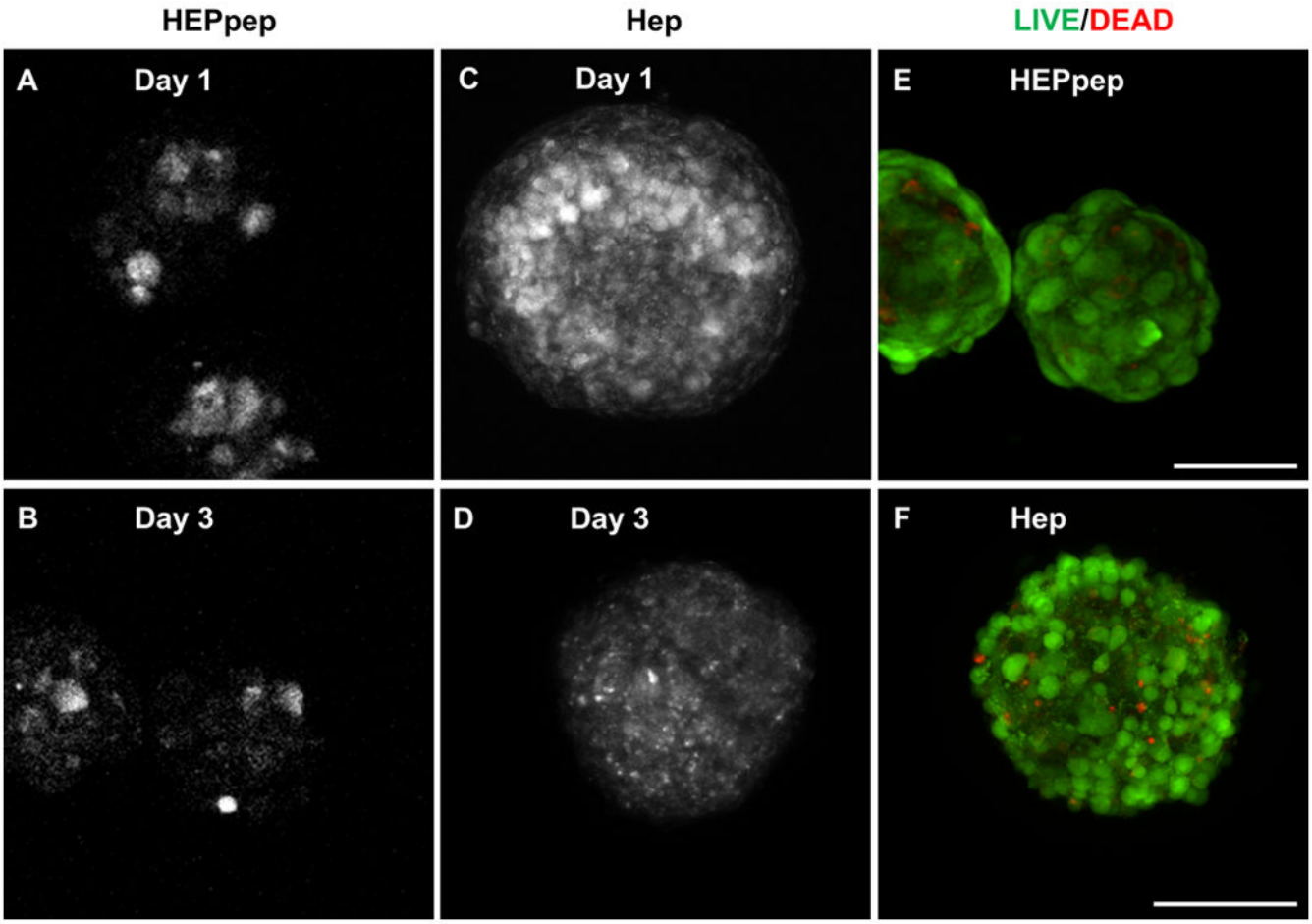

Figure 2.

HEPpep and Hep coating remains on cell surfaces for up to 3 days and does not negatively affect cell viability. Confocal images of HEPpep coating (greyscale) at (A) day 1 and (B) day 3. Hep coating (red) at (C) day 1, and (D) day 3. LIVE/DEAD of staining HEPpep coated (E) and Hep coated spheroids (F) spheroids at day 3. Scale bar = 100μm, n = 100 spheroids

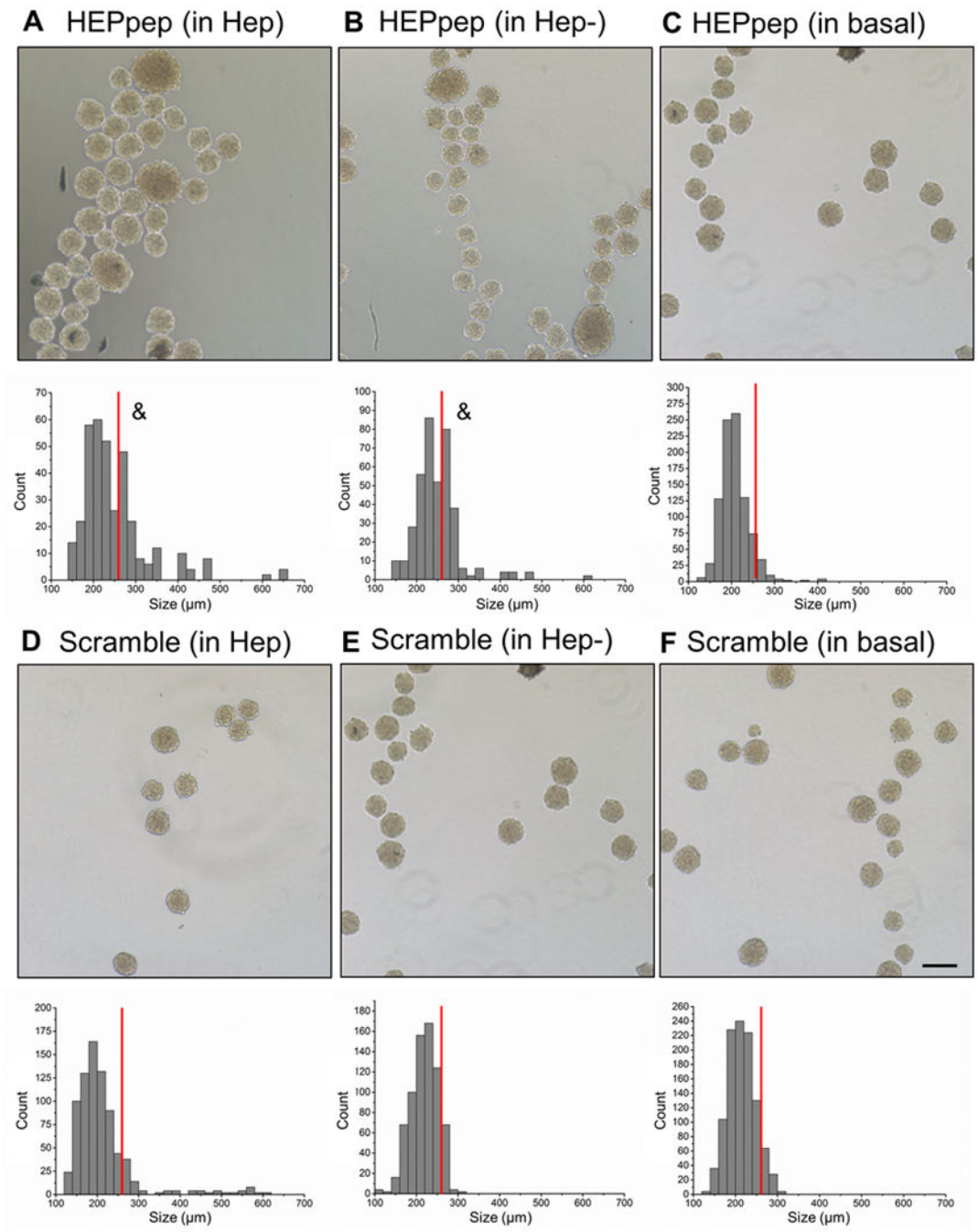

Figure 3.

HEPpep-coated spheroids increased in diameter when cultured for 24 hours in serum-free media containing soluble Hep or Hep-. Phase image (top) and histogram of aggregate diameters (bottom) of HEPpep-coated aggregates cultured in serum-free media containing (A) 5mg/mL heparin (B) 5mg/mL desulfated heparin or (C) basal conditions. Phase image (above) and histogram of aggregate diameters (below) of Scramble-coated aggregates cultured in serum-free media containing (D) 5mg/mL heparin, (E) 5mg/mL desulfated heparin, or (F) basal conditions. Scale bar = 100μm, n = ~1500 spheroids in total, red line

indicates cutoff size. & indicates significantly different from measurements above the cutoff size, $p<0.05$.

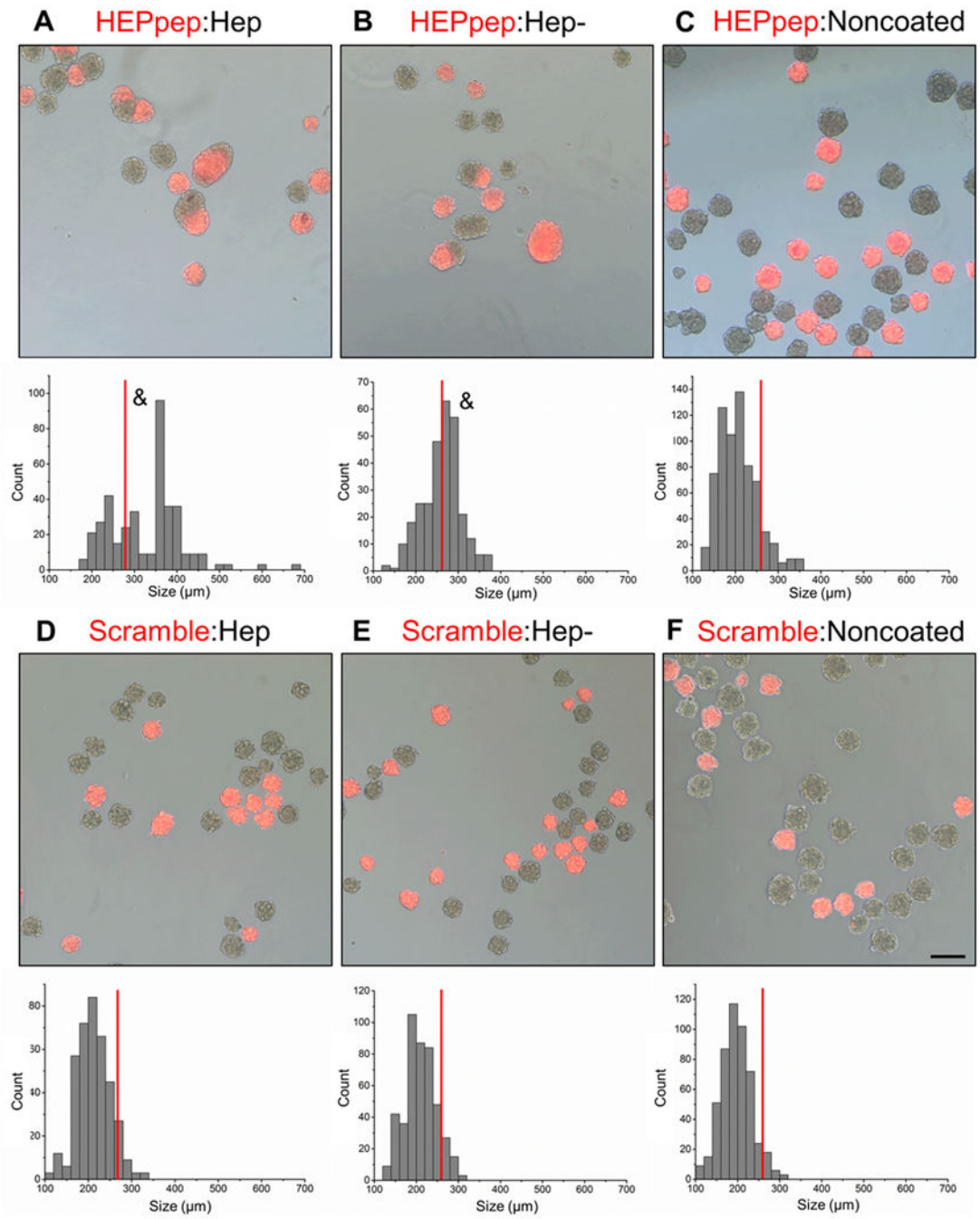

Figure 4.

HEPpep coated spheroids cultured with Hep coated spheroids exhibited larger assembled aggregates containing both cell populations after 24 hours. Merged phase and fluorescent image (top) showing peptide-coated fluorescent and non-fluorescent GAG-coated spheroids with histogram of aggregate diameters (bottom) (A-F; labels written as peptide-coating:GAG-coating). Scale bar = 100μm, n = ~1500 spheroids in total, red line indicates

cutoff size. & indicates significantly different from measurements above the cutoff size, $p<0.05$.

Table 1.

Resampled percentage of spheroids with diameters above cutoff size for HEPpep and Scramble-coated spheroids cultured in media containing GAGs in solution.

Group	Percentage Above Cutoff Size
HEPpep (in Hep)	34 ± 6% *
HEPPpep (in Hep-)	37 ± 5% *
HEPpep (in basal)	6 ± 5% ^
Scramble (in Hep)	13 ± 7% ^
Scramble (in Hep-)	10 ± 2% ^
Scramble (in basal)	8 ± 6% ^

* indicates significantly different from the percentage calculated from control populations

^ indicates significantly different from the percentage calculated from HEPpep (in Hep) population, $p<0.05$.

Table 2.

Resampled percentage of spheroids with diameters above cutoff size for peptide-coated spheroids cultured with GAG-coated spheroids.

Group	Percentage Above Cutoff Size
HEPpep:Hep	70 ± 11% *
HEPpep:Hep-	27 ± 4% *^
HEPpep:Noncoated	12 ± 5% ^
Scramble:Hep	10 ± 4% ^
Scramble:Hep-	9 ± 6% ^
Scramble:Noncoated	6 ± 2% ^

* indicates significantly different from the percentage calculated from control populations

^ indicates significantly different from the percentage calculated from HEPpep:Hep population, $p<0.05$.